Measurement of the V-T Energy Transfer Rates of Highly Excited $^2A_1$ NO_2

Troy L. Mazely†, Randall R, FriedI*, and Stanley P. Sander
Jet Propulsion Laboratory
California Institute of Technology
4800 Oak Grove Drive
Pasadena, CA 91109

Production of electronic ground state N02 (2A 1) from 248 nm photolysis of HN03 was detected by laser induced fluorescence (LIF). A growth in the LIF signal was observed following the photolysis and has been interpreted as the relaxation of N02 through the higher vibrational levels of the X(^{2}A 1) state; an energy region where the probe laser photodissociates the N02 instead of inducing fluorescence. The rate coefficients for N02 relaxation through these high vibrational levels were determined by fits of time resolved LIF signal to a stepladder kinetic model. The results of the kinetic analysis suggest that the observed relaxation begins at the ^{2}132 threshold near 9500 cm^{-1} and extends downward through approximately 5 vibrational levels of the ground electronic surface, The derived quenching rate coefficients (in units of 10-12 cm^3 molecule^{-1} s-]) are 0.51 ± 0.05, 1.03:0.1, 1.4 ± 0,2, 2.6 ± 0.6, and 8.7 ± 1.1 for Ar, He, N2, 02, and $C0_2$ collision partners, respectively. The discrepancies between these coefficients and previous literature values are rationalized in terms of a dependence of the vibrational relaxation rate on total internal energy.

†NASA/NRC Resident Research Associate

Introduction

The visible absorption and fluorescence spectra of N02, extending from 400 nm to beyond 700 nm, are quite complicated due to the mixing between the high vibrational levels of the X(2A $_1$) electronic state with the $A(^2B_2)$ and, to a lesser degree, the B(2I31) electronic states. [1] The extensive mixing between these electronic levels has made vibrational state specification of N02 difficult near, and beyond, the $^2B_2$ threshold which occurs approximately 9500 cm^{-1} above the ground state.[2]

Attempts to simulate the relaxation kinetics of electronically excited N02 (NO_2^*) have often employed a simplified population distribution that involves a discrete set of equally spaced levels.[3,4] In these models, the NO_2^* is allowed to relax collisionally to adjacent excited states or decay radiatively directly to vibrational levels in the $^2A_1$ state. Above the $^2B_2$ threshold collisional quenching predominates over radiative decay provided the total pressure is above 50 mTorr.5 Near the 2B2 threshold, electronic energy is transferred to the vibrational modes of the 2A] state; the resulting electronic ground state NO_2 is highly vibrationally excited ($NO_2^\dagger$). A change in the relaxation mechanism occurs as the excited NO_2 acquires more $^2A_1$ character because the deactivation is through well defined vibrational states of the ground electronic manifold instead of through a dense manifold of mixed electronic and vibronic states.

Experimental attempts to investigate the kinetics of NO_2 relaxation have relied mainly on observations of excited NO_2 emission, Measurements of visible emission lifetimes following optical excitation of NO_2, for instance, have led to a greater understanding of the electronic relaxation of NO_2^*.[3,6-13] Rate coefficients for electronic quenching of NO_2^* have been measured to be roughly gas kinetic, i.e. 10-10 cm^3 molecule-l s^{-1}, with only a slight dependence on the collision partner.

Vibrational deactivation of electronic ground state N02 has been investigated by a number of techniques. The earliest attempts involved monitoring the time resolved infrared chemiluminescence of $NO_2^{\dagger}$ arising from the reaction of NO with both O and 03. By measuring the emission in the 3.7 μm band of N02, Golde and Kaufman[14] estimated a rate coefficient for the vibrational relaxation of N02 in an Ar carrier gas of approximately 6 x 10-14 cm3 molecule-1 s-1. Although their technique could not yield a precise absolute rate coefficient, it provided meaningful relative rates as a function of buffer gas. Reported values were 55 ± 35, 40 ± 25, 5 ± 2, 2.0 ± 0.5, and 1 for N02, NO, 02, N2, and Ar, respectively. Unlike the electronic relaxation of N02, the Golde and Kaufman results demonstrate that vibrational relaxation is strongly dependent on the collision partner.

Vibrational relaxation has also been studied by observing infrared emission from optically excited N02. McAndrew et al. [15] inferred vibrational relaxation rate coefficients by measuring the time dependence of various infrared emission bands of N02. Based on a multiparameter kinetic fit of the emission in the 6.1-6.8 μm region ($\Delta v_3 = 1$ transitions), a vibrational quenching rate coefficient of (1.8 ± 0.6) x 10-13 cm3 molecule-1 s-1 was reported for He. Relative to the rate coefficient in He, the rates in N02, C02, and Xe were determined to be 18 ± 9, 15 ± 8, and 1.8 ± 0.8, respectively. The internal energy distribution of the N02 emitting in this band was not derived; presumably the emission contained contributions from a range of excited vibrational levels in the v3 manifold. Larger quenching rate coefficients were derived from emission in the 3-4 μm region, however, most of the signal in this region was attributed to electronic rather than vibrational components of the relaxation.

A method to probe relaxation of low-lying vibrational levels has been developed by Toselli et al. [16] They applied thermal lensing to study N02 vibrational relaxation following optical excitation. A rate coefficient of (5.1 ± 1.0) x 10-14 cm^3 $molecule^{-1}$ s^{-1} was derived for the relaxation of NO_2 (01 O) in Ar.

Theoretical models of V-T relaxation generally predict that the relaxation rate coefficient scales with total internal energy.q} 17-18 The model of Schwartz, Slawsky, and Herzfeld (SSH theory)[18] predicts that the relaxation rate should be directly proportional to the vibrational quantum number of the initial level. Recently, Adler-Golden[4] has presented a treatment specifically for N02 in which a density of states argument was employed to obtain a numeric expression for the relaxation rate coefficient as a function of the excess energy of the N02. Parameterization of the derived "expressions was made by combining existing data on the relaxation of N02. The results of this model predict a stronger dependence of the N02 relaxation rate on internal energy than SSH theory.

In this study we have obtained information on the vibrational relaxation of N02 at energies near the $^2B_2$ threshold by using HN03 photolysis as a convenient source of excited N02. The photolysis of HNO_3 has been extensively studied at a variety of wavelengths. 19-31 Although many mechanistic details remain uncertain regarding the photolysis products of HN03, especially as a function of wavelength, Reaction 1

$$HNO3 + h\nu \text{ ----> } OH + NO_2 \qquad (1)$$

is believed to be the only channel accessed at 248 nm. The deposition of the available excess energy after photolysis, ≈ 24,000 cm-l> into the OH and N02 photofragments has been studied by a number of investigators. Jacobs et al.[26], Schutter and Kleinermanns.[27], Likar et al.[28] and August et al.[29] utilized UV laser induced fluorescence to probe the nascent OH rotational and vibrational population distributions. These studies set 5°/0 as an upper limit of the amount of excess energy deposited into OH vibration and rotation. Oh et al.[30] observed visible emission from nascent N02 and suggested that a significant fraction of the N02 photoproduct is electronically excited. The internal energy of the nascent N02* photoproduct has been characterized by Miller.[31] The distribution is broad and ranges from 12,000 cm^{-1} to 23,000 cm^{-1} of internal energy with a maximum at approximately 16,000 cm^{-1} for photolysis at 248 nm. These energies, which are well above the threshold of the $^2B_2$ state, indicate that the nascent N02 is completely electronically excited.

We have utilized the technique of LIF as a diagnostic for N02. Since the threshold for photodissociation of N02 is at 25,100 cm-l, the photon energy of the probe laser employed in this study (19,600 cm^{-1}) is sufficient to induce photodissociation of all N02 molecules containing more than approximately 5500 cm^{-1} of internal energy.[5] Since the nascent N02 population is at energies above this value no initial LIF signal is expected and detection of N02 by LIF occurs only *after* the nascent population relaxes below 5500 cm^{-1}. We have analyzed the time delay in LIF detection of N02 following HN03 photolysis in order to quantify the kinetics of the N02 relaxation process between 9500 cm^{-1} and 5500 cm^{-1}.

Experimental

A schematic of the experimental apparatus is shown in figure 1. HN03 vapor was introduced into the flowing system by passing a carrier gas (He, Ar, N2, 02, or C02) through a bubbler containing pure liquid HN03. The HN03 was synthesized by collecting the vacuum distillate of a 50:50 by volume mixture of 95% H2S04 with $NaNO_3$. The HN03 was maintained at 0° C by placing the bubbler in an ice bath. The HN03 vapor concentration was determined by optical absorption at 254 nm in a 50 cm long absorption cell upstream of a teflon needle valve (Gilmont). The HN03 concentrations derived from the optical measurements agreed well with estimates based on the known vapor pressure of HN03. The pressures in the bubbler and absorption cell were controlled by the needle valve and monitored with an MKS Baratron capacitance manometer. All flows rates were determined using calibrated flow meters (Hastings).

The HN03 concentration in the quartz photolysis cell was reduced relative to the bubbler by injection of additional buffer gas in an upstream mixing region. The concentration of HNO_3 in the photolysis cell ranged between (0,08 -50.) x 1014 molecule cm-3 at total pressures between 0.5 to 10.0 Torr. The flow rate into the cell was varied between 250 to

4000 seem to insure complete flushing of the photolytic products between photolysis laser shots.

An excimer laser (Questek Model 2240) operating at 248 nm and at a pulse repetition rate of 20-30 Hz was used to photolyze HN03. The output of the excimer was weakly focused with a 2000 cm focal length lens. The pump laser optical path through the photolysis cell was defined by 0.86 cm diameter entrance and exit irises. The energy density of the excimer laser ranged from 25 to 150 mJ/cm^2 per pulse and was monitored with a Joule meter (Scientech P50). Under these conditions the photolytic signal was observed to be linear with laser pulse energy. The fractional dissociation of HN03 by each excimer laser pulse was estimated to be $\approx$ O. 10/0 based on the HN03 absorption cross section at 248 nm and a typical excimer laser fluence of 50 mJ/cm^2.

A 15 Watt, pulsed copper vapor laser (CVL: Oxford model CU1 5A) with a tunable repetition frequency between 6 to 20 kHz was utilized to probe for generated N02 by LIF. The 578 nm output from the CVL was eliminated by passage of the beam through two short wave pass filters, The transmitted 511 nm line was directed through a telescope to reduce the diameter of the beam. The weakly convergent beam was then passed through two irises and sent to the photolysis cell, The fraction of $N0_2$ excited by each probe pulse was estimated to be 0.05%. For some experiments the CVL was replaced by a 10 Hz, 150 mW Nd:YAG laser (Quanta-Ray DCR-1). The optical path of the 532 nm output of the Nd:Yag was similar to that of the CVL.

The LIF signal was detected by a cooled photomultiplier tube (PMT: Burle C3 1034-02) that was oriented orthogonal to the laser beam axes. The LIF signal was amplified, discriminated, and counted on a multi-channel scaler card (MCS: Canberra Accuspec) with a bin width of 5 μs. A 550 nm long pass filter was placed in front of the PMT to block excimer and CVL laser scatter. A set of experiments were performed that verified that the detected LIF signal was linearly dependent on both the probe laser pulse energy and the N02 number density, Using the CVL, a LIF detection sensitivity of approximately 3 x 109 N02 cm^{-3} was

achieved with signal averaging of 2.5 x 104 CVL pulses (≈ 1-2 seconds total time). Because of its higher pulse energy, the Nd:YAG probe provided a single pulse sensitivity to N02 over ten times greater than the CVL. However, the sensitivity of the CVL system per unit time is much greater than the Nd :YAG scheme because of its higher average power.

The timing and synchronization of the two lasers were controlled by a master clock (6-20 kHz), a frequency divider circuit, and two delay generators. The master clock pulses were used to trigger the CVL and the appropriately delayed" low frequency (20-30 Hz) outputs of the frequency divider were used to trigger the excimer and the MCS data collection. This arrangement allowed for selection of a wide range of delay times between the excimer laser pulse, the copper vapor laser pulse, and the signal collection.

One unique advantage of the current design was related to the employment of a CVL as the probe laser. Because of its high repetition frequency, the CVL sampled the reactor contents every 50-150 μs. Consequently, the temporal evolution of photolytic products from each excimer pulse could be monitored in real time long enough and with sufficient temporal resolution to characterize both the photodissociation yield and molecular diffusion out of the viewing zone. This information aided in determining the background probe signal and in ensuring that the photolytic products have completely left the viewing zone before the next excimer pulse. The large data return eliminated the need to systematically vary the triggering delays between the pump and the probe lasers for most experiments.

Results and Discussion

Miller et. al.31 have deduced that the majority of N02 produced from 248 nm photolysis of HNO_3 is initially in the ^{2}132 state, We have verified their conclusion by quantitatively detecting the spontaneous visible emission that accompanies HN03 photolysis. The intensity and frequency range of the observed excimer induced fluorescence (EIF) is

qualitatively similar to that observed by Oh et al.[30] and Miller et. al.[31] and attributed by them to emission from N02*. From our experimental observations of the EIF we have estimated that the quantum yield for N02* production from 248 nm photolysis of HN03 is greater than 0,6.

The temporal duration of the EIF was found to be less than 5 μs (one channel width of the multichannel scaler) at all experimental pressures (1 - 10 Torr). This observed upper limit is consistent with the collisional lifetime that we calculate based on published values of the collision-free NO_2^* lifetime (≈ 50 μs) and collisional quenching constants (≈ 6 x 105 $Torr^{-1}$ s^{-1} in Ar). The relatively short observed EIF lifetime reflects the fact that, under the present experimental conditions, relaxation of N02* occurs predominately by stepwise collisional quenching rather than radiative decay.

The time scale for the establishment of the initial distribution of $NO_2^\dagger$ is the same as for the decay of the EIF, i.e. less than 5 μs following the photolysis pulse. The energy distribution of the $NO_2^\dagger$ after a few microseconds is relatively narrow, consisting of a few highly excited vibrational levels near the $^2B_2$ threshold, This conclusion holds regardless of the nascent energy distribution of the N02* produced from HNO_3 photolysis since the collisional quenching rates for $^2B_2$ N02 are orders of magnitude larger than for $^2A_1$ N02.

Detection of the photolytically generated $NO_2^\dagger$ by LIF can begin only when the sum of the probe laser energy and the N02 internal energy is less than the N02 dissociation energy of 25,100 cm-l. Consequently, fluorescence induced from the 511 nm (19,600 cm-1) probe occurs only when the N02 internal energy is less than 5500 cm^{-1}. In order to properly interpret the observed N02 LIF it was necessary to characterize the dependence of LIF sensitivity on N02 internal energy for energies below 5500 cm^{-1}. The diffuseness of the visible N02 absorption spectrum suggests, in accordance with the Franck-Condon principle, that the overlap between the $^2B_2$ and $^2A_1$ states is a slowly varying function of vibrational level. A quantitative estimate of the Frank-Condon overlap integrals between these electronic levels of N02 was made using the model of Rosenstock and Sharp32 and the associated

computer code of Yamaguchi et al.[33] For 511 nm probe excitation, the overlap integrals were nearly identical for both vibrationally cold N02 and N02 with up to two quanta of vibrational energy in any of the three modes, The calculation was limited to two vibrational quanta by computer code restrictions, nevertheless, the analysis strongly suggests that, provided the total energy is not beyond the thermochemical threshold for the dissociation of N02, the LIF signal will be relatively independent of the degree of vibrational excitation of the NO_2. Accordingly, the LIF technique is uniformly sensitive to all ground state N02 molecules with less than 5500 cm^{-1} of internal energy and is insensitive to N02 above that energy level. Figure 2 illustrates the relationship between the relaxation of N02 and the appropriate regions where the relaxation is being followed.

N02 fluorescence data was collected under a range of pressures from 1-10 Torr and for a variety of different buffer gases, The temporal behavior of the observed LIF could be analyzed in terms of the following three processes: 1) an initial LIF signal that was due to nascent N02 with internal energies less than 5500 cm^{-1}; 2) a source of LIF signal that was due to relaxation of $NO_2^{\dagger}$ from levels above 5500 cm^{-1} of internal energy to levels below 5500 cm^{-1}; 3) a decay of the LIF signal that was due to the loss of N02 from the viewing zone because of diffusion, bulk gas flow, and secondary chemistry.

Analysis of low pressure data revealed that, the amount of directly produced N02 with energy less than 5500 cm-l is small. This finding is consistent with other studies where the nascent N02 population from HN03 photolysis was measured,[31] Consequent y, process 1 was neglected as a source of LIF signal, The loss of N02 from the viewing zone (process 3), was characterized by analysis of LIF data taken at higher buffer gas pressures. Under these pressure conditions the vibrational relaxation process, which produces the LIF signal, was complete before LIF data was recorded, i.e $t < 10\ \mu s$. Accordingly, the temporal behavior of the LIF after the first probe laser shot was dictated solely by process 3. The observed loss of N02 was well described by the following equation:

$$[NO_2(t)] = A\ e^{-k_{loss}\, t}, \qquad (2)$$

where $[NO_2(t)]$ is the N02 concentrate ion and k_{loss} is a rate describing the loss of N02 from the viewing zone due to diffusion, gas flow, and secondary chemical removal. This expression has been applied successfully to a number of photolytically generated radicals and molecules.[34] In the present experiments the complete temporal evolution of the LIF signals were well described by Equation 2 for every buffer gas employed when the total pressure was greater than 6 Torr. Measured loss rates were less than 500 s^{-1} and were, as expected for diffusion controlled processes, inversely dependent on the total pressure,

At lower total pressures, the production of LIF signal due to relaxation of $NO_2^{\dagger}$ (process 2) became observable. The maximum observable rate of LIF growth, as defined by the detection electronics, was on the order of 105 s-1. The rate of signal growth was readily observed to depend on the buffer gas (see Figure 3), This latter observation supports the assumption that the LIF production is related to a vibrational quenching mechanism rather than some alternative explanation such as secondary chemical production of N02.

Three kinetic models were applied to the experimental LIF data in order to estimate the quenching rate of the generated $NO_2^{\dagger}$. The simplest approach employed resembles the more detailed method of Donnelly et al.3 which was used to explain the collisional quenching from the ^{2}132 levels of N02. The treatment consists of a manifold of n equally spaced levels with equivalent quenching rate coefficients bet ween the adjacent levels. All of the initially generated N02 is assumed to be populated in one level which relaxes stepwise to the ground state. The model is fit to the data by varying the number of levels and the magnitude of the quenching rate coefficient. The solution is given by

$$\text{I. IF(t)} = \text{LIF}(0)\left[1 - e^{-k_q t}\sum_{j=0}^{n-2}\frac{(k_q t)^j}{j!}\right) \qquad (3)$$

where k_q is the first order relaxation rate coefficient and I. IF(t) is the fluorescence signal arising from N02 with internal energy less than 5500 cm-1. In order to account for the loss of the N02, the product of Equation 2 and 3 was applied to the data, i.e.

$$LIF(t) = LIF(0)\left(1 - e^{-k_q t}\sum_{j=0}^{n-2}\frac{(k_q t)^j}{j!}\right)e^{-k_{loss}t}. \qquad (4)$$

The other kinetic models that were applied to the data are due to Adler-Golden[4], and Schwartz, Slawsky, and Herzfeld (SSH).[18] The Adler-Golden model incorporates a quadratic (second order) dependence of the quenching rate coefficient on the excess energy of the N02, whereas the model developed from SSH theory incorporates a linear (first order) dependence of the rate coefficient on the excess energy. Since the model developed above has no energy dependence in the rate coefficients (zero order), a comparison of all three models to the data lends further insight into the actual energy dependence of the relaxation through these high lying vibrational states.

Figure 4 shows the temporal profile of the LIF signal following HN03 photolysis in an Ar buffer at a total pressure of 1.5 Torr. The values of k_q and k_{loss} were determined as a function of total number of levels by fitting the entire temporal profile (25 μs to 1000 μs) to Equation 4. The derived value of k_{loss} was independent of both the number of levels employed and k_q. Because the total quenching rates, i.e. k_q M, were, under all conditions, 1 to 2 orders of magnitude faster than k_{loss}, these two parameters were numerically uncoupled in the fitting routine.

The simple "zero order" model fit to the data is shown in figure 4, The fit improves as the number of levels are increased from 2 to 5, but degrades when more than 6 levels are incorporated. Adding more levels to the model effectively delays the initial growth of the signal because the system is relaxing through more states before reaching the lower vibrational levels where the LIF is observed. The inclusion of additional levels is accompanied by slightly larger calculated rate coefficients. Model fits were optimized for a number of data sets obtained under a range of experimental conditions. The number of vibrational levels required in the fits varied between 4 and 6. For comparison, the number of N02 vibrational levels that are contained within the experimentally defined 4000 cm^{-1} energy window (9500 cm^{-1} to 5500 cm^{-1}) are 3, 5, and 2 for the ν_1 (1318 cm^{-1}), v2 (749.65 cm^{-1}), and v3 (1617.8 cm^{-1})

manifolds, respectively.35 This comparison suggests that the vibrational relaxation occurs via the manifold with the highest density of levels (i.e. v2). This proposed mechanism is consistent with predictions based on energy gap models.

The application of the "first order" SSH model to the data resulted in rate coefficients that are virtually identical to those derived from the "zero order" model fit. This agreement reflects the approximate constancy" of rate coefficients predicted by SSH theory for high vibrational quantum numbers. The application of the "second order" Adler-Golden model to the data resulted in significantly worse fits compared to the other two. Upon analysis of these fits it was clear that the quadratic rate coefficient dependence on vibrational level is too strong to properly mimic the experimental observations.

The first order relaxation rates derived from the "zero order" model are linear with pressure as shown in Figure 5, The slope of the fitted line gives a value of (4.5+ 0.4) x 10^{-1}3 cm^3 $molecule^{-1}$ s^{-1} for the bimolecular quenching rate coefficient in Ar, where the quoted error is at the $\pm 1\sigma$ precision limit. An average of data acquired at different total pressures yields a quenching rate coefficient of (5.1 ± 0.5) x 10-13 cm3 $molecule^{-1}$ s^{-1} for relaxation in Ar. All of the other carrier gases were found to be more efficient than Ar in relaxing the N02 through the high vibrational states. The results are summarized in Table I along with previous literature results.

The absolute rate coefficients obtained in the present study are larger than the previously reported values. Refs. 14 and 16 reported the slowest relaxation rates. The absolute rate coefficient from Ref. 14 is an estimate based on a comparison to other data and no uncertainty on this value was presented. The relaxation rate in Ref. 16 represents deactivation of $NO_2(01O)$, i.e. E_{int} = 750 cm-lo The results of Ref. 15, in which relaxation was monitored through the entire vibrational manifold, i.e. $Ei_{nt} \leq 9500$ cm^{-1}, are intermediate between the present values and those of Ref. 16. The present rate coefficients, which correspond to relaxation solely in the region of 5500 $cm^{-1} \leq Ei_{nt} \leq 95OO$ cm^{-1}, continue a trend which can be rationalized in terms of a dependence of the rate coefficient on total internal

energy.

The relative rate coefficients agree well with literature values. The relative rates in Ar, N2, and 02 are, within the stated error, identical to those reported in Ref. 14. The ratio of the rates in C02 and He from Ref. 15 are within a factor of two of the present results and overlap one another within the cited precision.

Conclusion

The majority of N02 generated from photolysis of HN03 at 248 nm is electronically excited. The nascent N02* is rapidly redistributed by collisional deactivation into a relatively narrow energy region near the threshold of the 2B2 manifold near 9500 cm^{-1}. Quenching rate coefficients for relaxation through the higher vibrational levels of the $2A_1$ manifold were determined by a fit of LIF data to a simple stepwise kinetic mechanism. The model fits indicate that approximately 4 to 6 vibrational levels are involved in the deactivation of the N02 from a narrow distribution centered at 9500 cm^{-1} to levels below 5500 cm^{-1}. This finding suggests that the relaxation process occurs primarily through the v2 manifold. The measured vibrational relaxation rates were found to depend strongly on the collision partner. The derived rate coefficients are larger than in those studies where relaxation through lower vibrational states was probed. These results are consistent with theories that predict a dependence of the vibrational relaxation rate on total internal energy,

Acknowledgment: The research described in this paper was carried out at the Jet Propulsion Laboratory, California Institute of Technology, under contract to the National Aeronautics and Space Administration,

References

[1] K. Uehara and H. Sasada, *High Resolution Spectral Atlas of NO_2 559-597 nm* (Springer-Verlag, New York, 1985).

[2] A. Weaver, R. B. Metz, S. E. Bradforth, and D. M. Neumark, J, Chem. Phys. **90,** 2070 (1989).

[3] V. M. Donnelly, D. G. Keil, and F. Kaufman, J. Chem. Phys. 71,659 (1979).

[4] S. M. Adler-Golden, J. Phys. Chem. 93,684 (1989).

[5] H. Okabe, *Photochemistry of Small Molecules* (Wiley, New York, 1978).

[6] A. E. Douglas, J. Chem. Phys. 45, 1007 (1966).

[7] K. Sakurai and H. P. Broida, J. Chem. Phys. 50,2404 (1969).

[8] S. E. Schwartz and H. S. Johnston, J. Chem. Phys. **51,** 1286 (1969).

[9] V. M. Donnelly and F. Kaufman, J. Chem. Phys. 66,4100" (1977).

[10] V. M. Donnelly and F. Kaufman, J. Chem. Phys. **69,** 1456 (1978).

[11] C. H. (_'h_{en}, S. D. Kramer, D. W. Clark, and M. G. Payne, Chem. Phys. Lett. 65, 419 (1979).

[12] Cheshnovsky and A, Amirav, Chem. Phys. Lett. 109,368 (1984).

[13] C. Anastasi and D. U. Hancock, J. Chem. Soc., Faraday Trans. 284, 1697 (1988).

[14] M. F. Golde and F. Kaufman, Chem. Phys. Lett. 29, 480(19'74).

[15] J. J. F. McAndrew, J. M. Preses, R. E. Weston, Jr. and G. W. Flynn, J. Chem. Phys. **90,** 4772 (1989).

[16] B. M. Toselli, T. L. Walunas, and J. R. Barker, J. Chem. Phys. 92,4793 (1990).

[17] J. L. Hardwick, J, Mol. Spectros. 109, 85 (1985).

[18] R, N. Schwartz, Z. I. Slawsky, and K, F. Herzfeld, J. Chem. Phys. **20,** 1591 (1952).

[19] A. A. Turnipseed, G. L. Vaghjiani, J. E. Thompson, and A. R. Ravishankara, J. Chem. Phys. 96, 5887 (1992).

20 T. Berces and S. Forgeteg, Trans. Faraday Soc. 66,633 (1 970).

21 H. S. Johnston, S. -G. Chang, and G. Whitten, J. Phys. Chem. **78,** 1 (1974).

22 H. Okabe, J. Chem. Phys. 72,6642 (1980).

23 M. Suto and L. C. Lee, J. Chem. Phys. 81, 1294(1984).

24 G. S. Jolly, D. L. Singleton, D. J. McKenney, and G. Paraskevopoulos, J. Chem. Phys. 84, 6662 (1986).

25 R, D. Kenner, F, Rohrer, Th. Papenbrock, and F. Stuhl, J. Phys. Chem. **90, 1294** (1986).

26A, Jacobs, K. Kleinermanns, H. Kuge, and J. Wolfrum, J. Chem. Phys. 79,3162 (1983).

27 J. Schlutter and K. Kleinermanns, Chem. Phys. Lett. **192,94** (1992).

28 M. D. Likar, A. Sinha, T. M. Ticich. R. L. Vander Wal, and F. F. Crim, Ber. Bunseges Phys. Chem. 92,289 (1988).

29 J. August, M. Brouard, M. P. Docker, A. Hodgson, C. J. Milne, and J. P. Simons, Ber. Bunseges Phys. Chem. 92, 264(1988).

30 D. Oh, W. Sisk, A. Young, and H, Johnston J, Chem. Phys. 85,7146 (1986).

31 C. E. Miller, Ph.D. Dissertation, University of California, Berkeley (1991).

32 T. E. Sharp and H. M. Rosenstock, J. Chem. Phys. 41, 3453 (1964).

33 M, Yamaguchi, T. Momose, and T. Shida, J. Chem. Phys. **93,** 4211 (1 990).

34 H. H. Nelson and H. S. Johnston, J. Phys. Chem. **85,** 3891 (1981).

35 T. Shimanouchi, J. Phys. Chem. Ref. Data 6, 993, (1977).

Table I: Summary of experimental relaxation rate coefficients for NO_2†

	$k(10^{-13}$ cm^3 molecule-1 S-l)				k/k_{Ar}	
M	Ref. 14	Ref. 15	Ref. 16	This work	Ref. 14	This work
Ar	0.6*		O.51*.1O	5.1 ± 0.5	1.	1.
He		1.8 ± 0.6		10. ± 1.		2.0 ± 0.3
Xe		3.3 ± 0.9				
N2				14. * 2.	2.0 ± 0.5	2.7 ± 0.2
O_2				26. ± 6.	5. ± 2.	5. ± 1.
CO_2		27. * 12.		87. ± 11.		17. ± 3.
NO					40. ± 25.	
N02		33. * 12.			55. *35.	

* Estimate only

Figure Captions

Figure 1: Schematic of the experimental apparatus.

Figure 2: Relationship between the observed LIF signal and relaxation of N02. The nascent N02 distribution resulting from the photolysis of HN03 ranges from 12,000 cm^{-1} to the total available energy of 23,700 cm^{-1}. Collisional quenching of N02 electronic energy is rapid and occurs prior to the commencement of LIF measurements. As a result the NO_2 population distribution at the start of LIF measurements is concentrated near the ^{2}B2 threshold energy (9500 cm^{-1}). No LIF signal is observed from N02 with internal energy above 5500 cm-l because the probe laser induces dissociation rather than fluorescence. Below 5500 cm^{-1} of internal energy the Franck-Condon factors for N02 absorption of a probe laser photon are approximately equal. Accordingly, the temporal delay in the observation of LIF following HN03 photolysis can be related to the kinetic parameters associated with vibrational deactivation of highly excited (5500 cm-l < Hint< 9500 cm^{-1}) ground state N02.

Figure 3: Temporal dependence of N02 LIF signal in two different buffer gases. The total pressure is 2 Torr and the concentration of HNO_3 is 1.6 x 1014 molecule cm^{-3}. The filled circles are data taken in 02 and the fit to the data is from Equation 2 with k_{loss} = 1560 S-l. The open circles correspond to Ar and the fit is to a 5 level kinetic model (Equation 4) with k_{loss} = 1520 S-l and k_q = 5.3 × 10-13 cm^3 molecule-l s^{-1}.

Figure 4: Temporal profile of N02 LIF signal in Argon. Total pressure is 1.5 Torr and the HN03 concentration is 7.7 x 1013 molecule cm^{-3}. The dashed, solid, and dotted lines represent fits of Equation 3 to the data with 2, 5, and 10 levels, respectively. The diffusional loss parameter, k_{loss}, is fixed at 2100 s^{-1} and the rate coefficients in order of increasing number of levels are 3.7, 6.6, and 14.4 x 10-13 cm^3 molecule-l S-l .

Figure 5: The first order N02 vibrational quenching rates as a function of Ar pressure. The fractional concentration of HN03 in these runs is fixed at 2500 ppm. Each rate is determined from a fit of Equation 4, where n=5, to temporal profiles of N02 LIF, as shown in Figure 2. The solid line is a linear least square fit of the data. The slope of the line corresponds to a bimolecular quenching rate coefficient of (4.5 ± 0.4) x 10-13 cm^3 $molecule^{-1}$ s^{-1}.

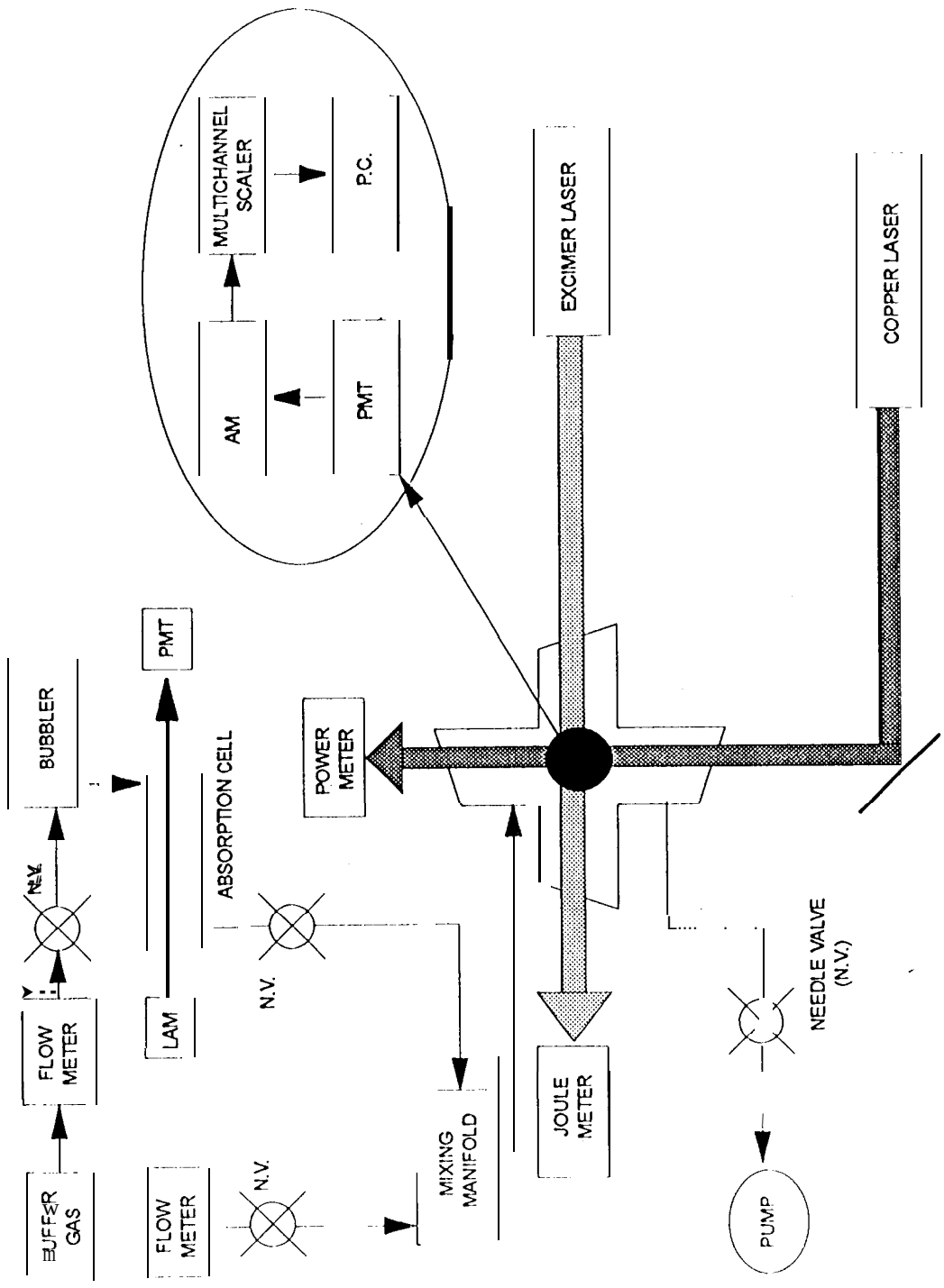

FIGURE 1

MARELY, FRIEDL, SANDER

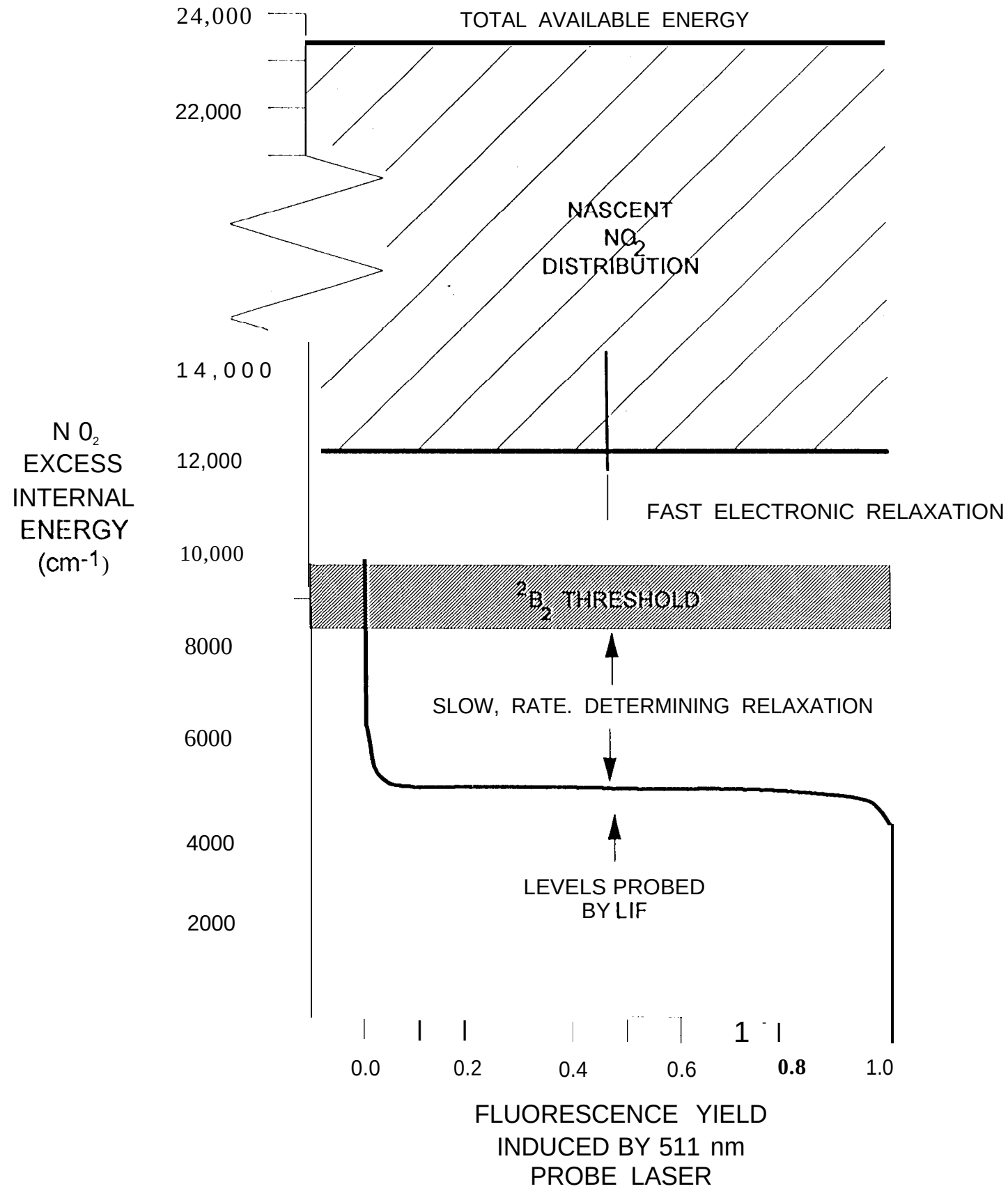

FIGURE 2

MAZELY, FRIEDL, SANDER

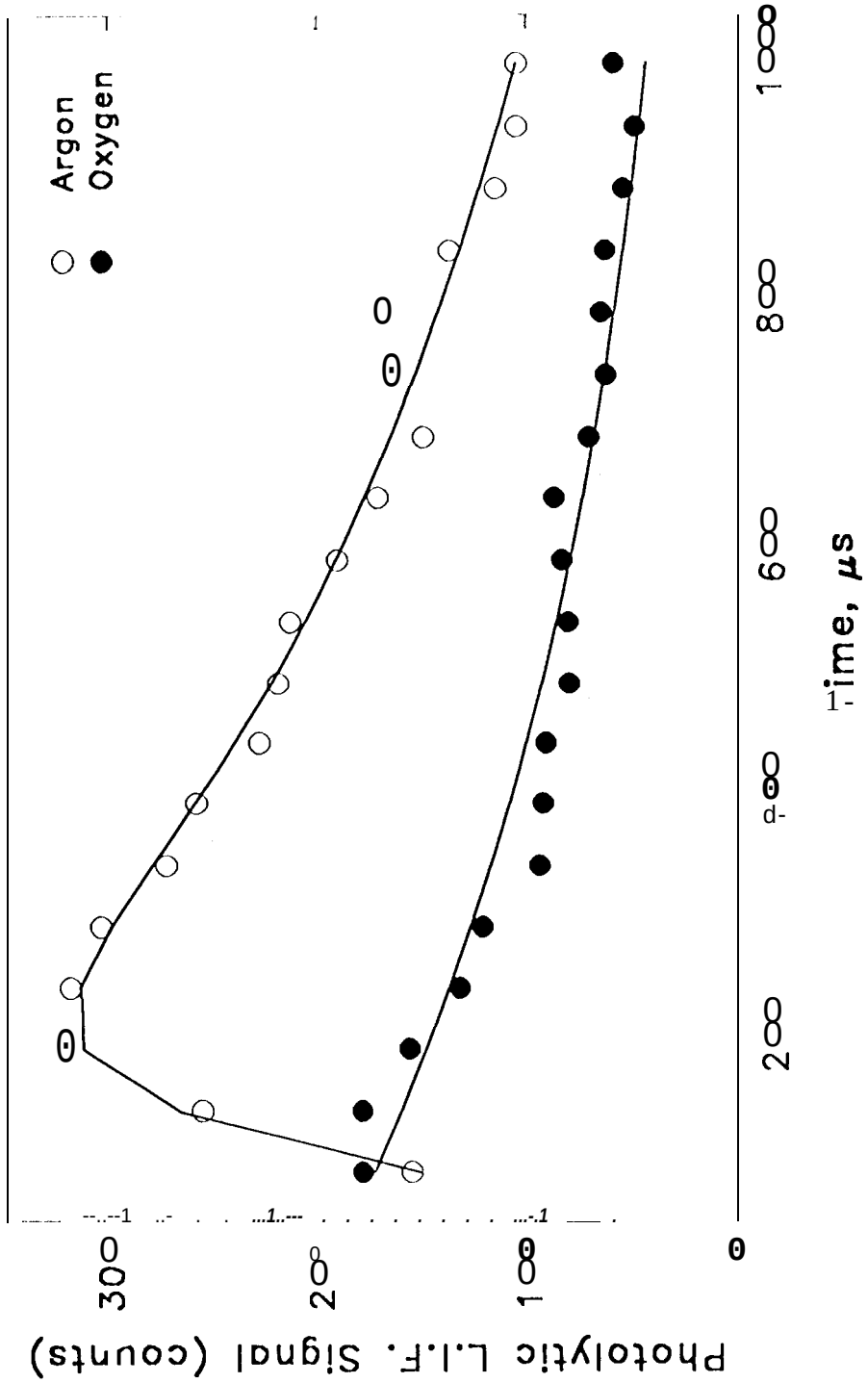

FIGURE 3

MARFIN FRIEDMAN JANDER

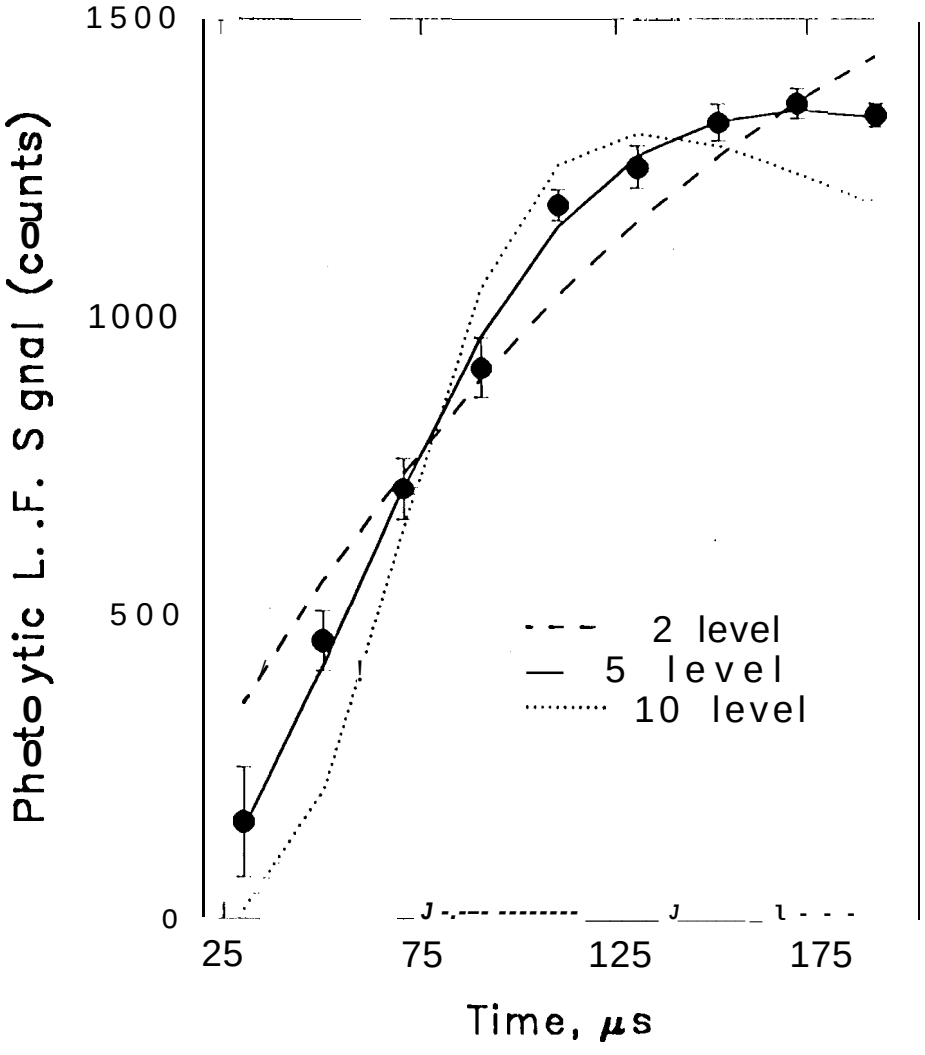

FIGURE 4

MAZELY, FRIEDL, SANDER

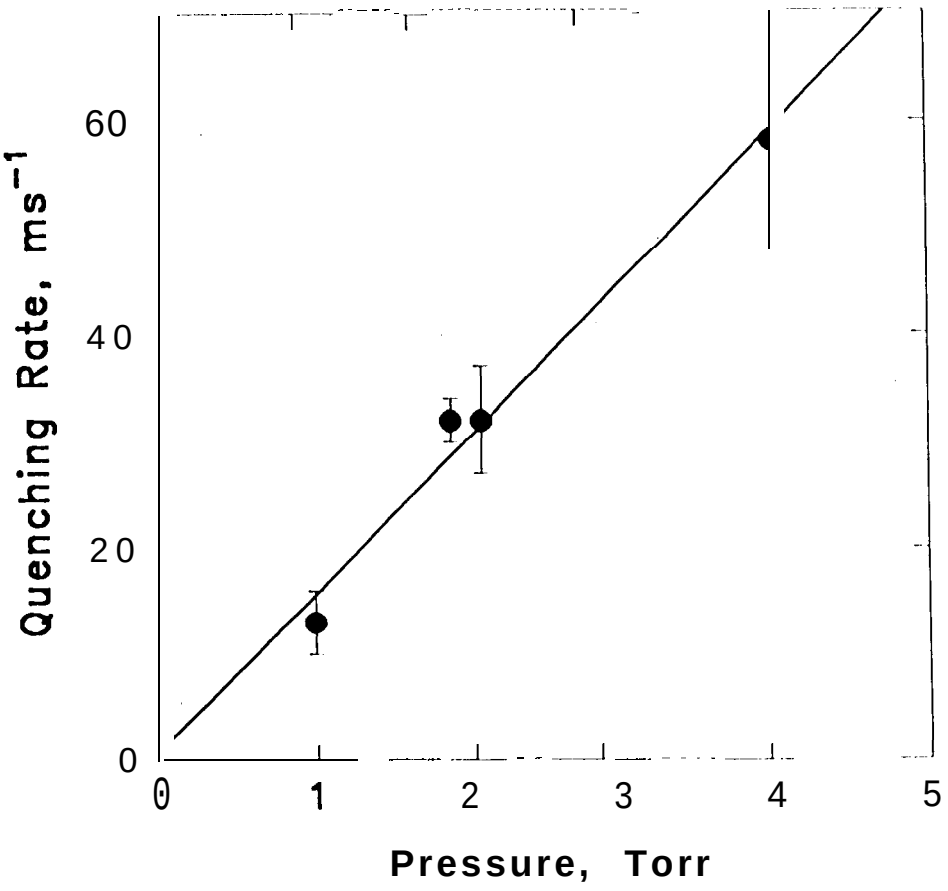

FIGURE 5

MAZELY, FRIEDL, SANDER